Journal of Advanced Joining Processes 9 (2024) 100172

Contents lists available at ScienceDirect

Journal of Advanced Joining Processes

journal homepage: www.sciencedirect.com/journal/journal-of-advanced-joining-processes

Experimental investigations on microstructure and mechanical properties of wall structure of SS309L using wire-arc additive manufacturing

Rakesh Chaudhari [a], Sakshum Khanna [b], Jay Vora [a,*], Vivek Patel [c,*]

[a] Department of Mechanical Engineering, School of Technology, Pandit Deendayal Energy University, Gandhinagar 382007, Gujarat, India
[b] School of Technology, Pandit Deendayal Energy University, Gandhinagar 382007, Gujarat, India
[c] Department of Engineering Science, University West, Trollhättan 46186, Sweden

ARTICLE INFO

Keywords:
Wire-arc additive manufacturing (WAAM)
SS309L
Mechanical properties
Wall Structure
Microstructure
GMAW

ABSTRACT

In present study, a wall structure of SS309L was constructed through Gas metal arc welding based Wire-arc additive manufacturing process. The wall structure of SS309L underwent investigation for microstructure and mechanical properties at three positions along the horizontal deposition direction. Mechanical assessments, including microhardness testing, impact testing, tensile testing, and fractography, were conducted at three positions of walls. Microstructure study has shown a fine granular structure in addition to colony of columnar dendrites in bottom section, a columnar dendrites in middle section, and a mix of dendritic structure with even coarser structures in top section. The mean microhardness values were observed to be 159 ± 4.21 HV, 162 ± 3.89 HV, and 168 ± 5.34 HV for the top, middle, and bottom sections, respectively. Results of impact testing for the wall structure indicated greater strength compared to wrought SS309L. The tensile strength of the built structure showed average values of yield strength, ultimate tensile strength, and elongation to be 409.33 ± 7.66 MPa, 556.66 ± 6.33 MPa, and 39.66 ± 2.33 %, respectively. In comparison, wrought 309 L steel typically exhibits tensile strengths in the range of 360–480 MPa for yield strength, 530–650 MPa for ultimate tensile strength, and 35–45 % elongation. Thus, the obtained tensile strength results for the wall structure fall within the range of tensile strength observed in wrought 309 L steel. Fractography of the tensile and impact specimens, as obtained through Scanning Electron Microscopy, revealed the superior ductility of the fabricated component. This study contributes valuable insights into the manufacturing of wall structure and their analysis regarding mechanical characteristics.

Introduction

Additive manufacturing (AM) system which forms a 3D structure by deposition of layer by layer has increased popularity due to their minimum production time, and less material wastage (Zahidin et al., 2023; Taheri et al., 2022). AM process protects around 50 % of manufacturing cost in comparison with the conventional processes (Korkmaz et al., 2022; Zhou et al., 2022). Thus, AM finds their applications in multiple sectors such as aerospace, automotive, medical, defence and several other areas (Nguyen et al., 2022; Rauch et al., 2021). Out of the three broad classifications of AM process such as sheet lamination, direct energy deposition (DED), and powder bed fusion, the DED technique provides additional benefits like higher deposition rate, and their ability to fabricate large metallic parts (Li et al., 2023; Piscopo and Iuliano, 2022; Chaudhari et al., 2023). The wire arc additive manufacturing (WAAM) process of DED utilizes wire feedstock as a source of energy (Hu et al., 2020; Shen et al., 2022). The rate of deposition for the WAAM process (3–8 kg/h) is significantly higher than the powder bed AM process (0.1–0.7 kg/h) (Williams et al., 2016; Kokare et al., 2023). Additionally, the WAAM process reduces the production cost as the manufacturing cost of metal wire is lower in comparison with metal powder (Derekar, 2018). WAAM process utilizes various arcs such as plasma arc welding, gas tungsten arc welding, and gas metal arc welding (GMAW). Among these arc and energy sources, the GMAW process exhibits a larger deposition rate which is 2–3 times greater than the other two processes (Chaudhari et al., 2022; Ilman et al., 2022). Also, the GMAW-based WAMM process displayed suitable mechanical properties, fabrication of large-scale components, and lower cost of equipment (Dinovitzer et al., 2019; Sinha et al., 2022). Babu et al. (2023) preferred GMAW process due to the higher deposition rate and high process

* Corresponding authors.
E-mail addresses: jay.vora@sot.pdpu.ac.in (J. Vora), vivek.patel@hv.se (V. Patel).

https://doi.org/10.1016/j.jajp.2023.100172

Available online 7 December 2023
2666-3309/© 2023 The Author(s). Published by Elsevier B.V. This is an open access article under the CC BY license (http://creativecommons.org/licenses/by/4.0/).

efficiency to control microstructure and mechanical properties of high strength steel. Müller et al. (2022) employed direct energy deposion method to fabricate a thin walled structure of high-strength steel structures.

In recently published studies, researchers have given more emphasis to analyzing the wall structure fabricated through the WAAM process for aluminium, stainless steels, titanium, and nickel-based alloys (Wang et al., 2019; Wu et al., 2018; Bajaj et al., 2020). Among the steels, a large number of studies were focused on low-carbon steels, 304 L, 308 L, and 316 L. Analysis of WAAM structure for microstructure and mechanical characteristics of SS309L has not been studied in depth. Fabrication of 3D structures through the WAAM process has gained a lot of attention for stainless steel (Zhang et al., 2022; Duarte, 2021). SS309L finds their use in multiple areas like aerospace industries, manufacturing, automobile, mining, and biomedical due to the excellent strength-to-weight ratio, higher corrosion resistance, better mechanical characteristics, and higher strength and durability (Israr and Buhl, 2023; Kimura et al., 2020). Due to their greater heat resistance properties, SS309L is also preferred in chemical, oil, gas and petrochemical sectors (Jin et al., 2020; Isquierdo et al., 2022). Owing to the presence of higher carbon content in SS309L, it can resist higher temperatures than other steels (Sohrabi et al., 2020).

Van Thao (2020) analyzed the quality of the wall structure fabricated through the GMAW based WAAM process of low-carbon steels. The results of the microstructure study have shown primary dendrites in the top section, granular structure in the middle section, and grains in the bottom section of the built structure. The hardness of the built structure was obtained within 164 to 192 HV, having its highest value in the top section as compared to the middle and bottom sections. They also verified the mechanical characteristics such as yield strength (YS), and ultimate tensile strength (UTS), and observed that the obtained properties were found to be comparable with other conventional processes. Thus, they concluded that the GMAW based WAAM process was suitable for the fabrication of SS parts. Chaudhari et al. (2022) employed GMAW based method to analyze the effect of WAAM variables such as voltage, travel speed, and wire feed speed of SS316L. A heat transfer search algorithm was utilized to optimize the output variables of bead height and bead width. The wall structure was effectively manufactured at optimized WAAM variables of voltage at 19 V, WFS at 5.50 m/min, and TS at 141 mm/min. Their findings have revealed that optimized parametric settings of WAAM variables were a vital factor in the manufacturing of built components.

Kumar et al. (2021) used GMAW-based WAAM process to characterize the mechanical properties and microstructure of steel structures. Results of their microstructure study has revealed fine grains of ferrite and bainitic structures at top section, courser grains at middle section, and finer grains with ferrite and pearlite structures at bottom section of the fabricated wall. In another study conducted by Vora et al. (2022), the GMAW process successfully fabricated a thin-walled structure of 2.25 Cr-1.0 Mo Steel. The obtained results have depicted that optimal process parameters were beneficial in the layer-on-layer deposition of weld beads. Mai et al. (2021) preferred the GMAW based WAAM process over the plasma arc, and gas tungsten arc based process owing to their larger rate of deposition. The thin-walled structure of SS308L was built by using optimum process variables. They characterized the microstructure and characteristics of the built structure. The microstructure study revealed the presence of two phases within the austenitic matrix of residual ferrite and columnar austenite dendrites. The mean value of microhardness (MH) of the built structure was found to be around 163 HV, and tensile strength was observed to be UTS of 552.95 MPa, YS of 352.69 MPa, and elongation (EL) of 13 % in the depositing direction. After comparing the mechanical properties of the built structure with wrought SS308L, they concluded that all characteristics fall within the range of wrought SS308L.

Vora et al. (2022) formed a thin-walled component through the GMAW process of 316 L. The component was built at optimized WAAM variables and thus it was observed to have seamless fusion and free from disbonding. Their findings have revealed the different microstructures in the various sections of the component showing vertical dendritic structure in the top section, columnar dendrites in the bottom section, and residual ferrite in the middle section. The means tensile strength with YS, UTS, and elongation of 512.53 MPa, 256.57 MPa, and 49.35 % respectively were obtained for the wall structure. These values fall within the range of the characteristics to that of wrought 316 L. MH and impact test results have also depicted superior strength as compared to wrought 316 L. Fractography results have revealed ductile fracture showing excellent strength of the fabricated component. Ji et al. (2017) analyzed the mechanical properties, and microstructure of SS304L specimens formed from WAAM process. Mai (2020) fabricated a thin muti-layered SS308L by employing the GMAW process. They investigated t the mechanical properties, and microstructure of the built component. Microstructure results revealed columnar dendrites in the built path. The MH value was observed to be within the value of 155–169 HV while, tensile strengths with YS, UTS, and EL were observed as 352 MPa, 552 MPa, and 54 % respectively in the horizontal direction.

To the best of the authors' knowledge, limited investigation has been carried out for analysis of WAAM structure for microstructure and mechanical properties of SS309L. The studied literature suggested that the fabrication of wall structure with desired mechanical characteristics can be obtained at optimized parametric settings of the GMAW-based WAAM process. In the present work, a wall structure of SS309L was fabricated on the SS316L substrate plate at optimized parametric settings. The built component of SS309L was investigated for microstructure, and mechanical properties at three positions along the horizontal depositing direction. Mechanical investigations of tensile testing, microhardness, impact test, and fractography have been conducted at three positions along the depositing direction. The obtained results were found to be vital for various industrial applications and also useful in case of conducting further research in the domain. The current study paves way for the successful implementation of WAAM technique for manufacturing of SS309L components particularly for critical applications such as nuclear reactors, powerplant valves/flanges etc. One of the key application of the study is also repair of existing broken or damaged parts rather than replacing them entirely.

Experimental procedures

Experimental plan

In the current study, SS309L metallic wire having a diameter of 1.2 mm was used to build a wall structure on the SS316L substrate plate (dimensions of 200 × 200 × 20 mm) by employing the GMAW based WAAM process. The chemical composition of the metallic wire and substrate plate is shown in Table 1. Fig. 1 depicts the experimental setup employed during the present study. The experimental setup consisted of key components such as a wire feeder, shielding gas, controllers, mixing chambers, and GMAW torch (PRO MIG-530). The WAAM setup has 220 × 220 × 500 mm of the built volume. The substrate plate of SS316L was fixed and the torch was utilized to deposit the wall structure on the plate. GMAW torch can move in all three axes for the material depositions. G-code programming was preferred to deliver response through the controller unit. For the heating and melting of metallic wire, the power source of COLTON iFLEX 350 was utilized.

In the past study conducted by authors, bead morphologies of GMAW-based WAAM process was investigated and optimized for bead height and bead width responses (Vora et al., 5147). Firstly, by using Box-behnken design at three variables (travel speed, gas mixture ratio, and voltage), experiments of single-layer deposition were perfomed. For all the trials, bead height and bead width responses were measured and validated statistically. The main aim of the study was to obtain optimal process parameters to fabricate wall structure. Persuant to this, bead

Table 1
Chemical elements of metallic wire and substrate plate (Vora et al., 5147).

Element	Cr	Ni	Mo	Mn	Si	C	P	S	N	Fe
Metallic wire (SS309L)	22–25	12–15	–	2	1	0.2	0.045	0.03	–	Balance
Substrate (SS316L)	17.09	10.61	2.38	1.17	0.59	0.013	0.011	0.011	0.09	Balance

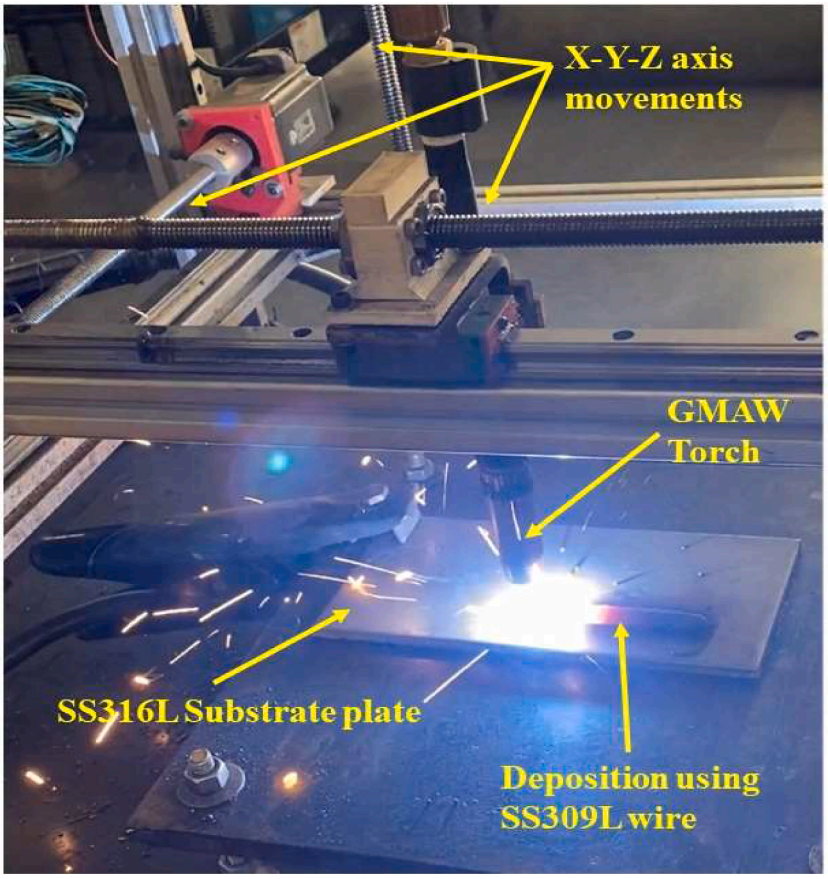

Fig. 1. Experimental setup of the GMAW-based WAAM process.

height and bead width were considered as higher-the better and lower-the better responses respectively during the optimization. A metaheuristic optimization technique of Passing vehicle search (PVS) algorithm was employed to find the optimized process variable owing to their advantages like easy to apply, fast, and establishes improved convergence for the desired outcome. By using simultaneous optimization, an optimized set of parameters was derived as shown in Table 2. Gas mixture ratio denoted the amount of CO_2 gas, while the remaining amount contains argon gas.

Testing and characterization

The wall structure of SS309L was examined for microstructure, and mechanical properties at across the built structure in multiple locations. The layer-on-layer deposition of wall structure has been manufactured by using 180-degree turns of SS309L wire to obtain better precision. The experiments were reproduced three times, and average value of the obtained results was considered for the analysis purpose. To cool the built parts, minimize the residual stresses, and transfer the collected heat, a dwell period of 60 s was retained during the adjacent layers of the built structure.

Table 2
Optimal conditions of GMAW-based WAAM process (Vora et al., 5147).

Input variables	Value
Voltage (V)	22 V
Gas Mixture Ratio (GMR)	3
Travel speed (TS)	*20* mm/s
Gas flow rate	15 L/min
Arc length	3 mm
Weld bead length	150 mm

Fig. 2 depicts a schematic of built components showing the locations for different characterizations along with the dimensions. The microstructure, and mechanical characteristics of structure was analyzed at three positions along the depositing direction. Multiple locations of the top, middle and bottom of the built structure which were denoted by TS-1, TS-2, and TS-3 for tensile test, I-1, I-2, and I-3 for impact test, and MS-1, MS-2, MS-3 for microstructure respectively. Wire-electric discharge machine (WEDM) set-up was employed to remove the built structure from the substrate plate, and also to prepare the samples for multiple characterizations.

The specimens required for microstructures were initially polished by using abrasive papers of different grit sizes, and later on, a mirror finish was obtained by polishing them using the diamond polishing agent of 2 μm size. The components were subsequently etched for 60 s in a solution of 10 mL of Nitric Acid (HNO_3), 20 mL of Hydrochloric Acid (HCL), and 30 mL of water (Van et al., 2021). The examination of

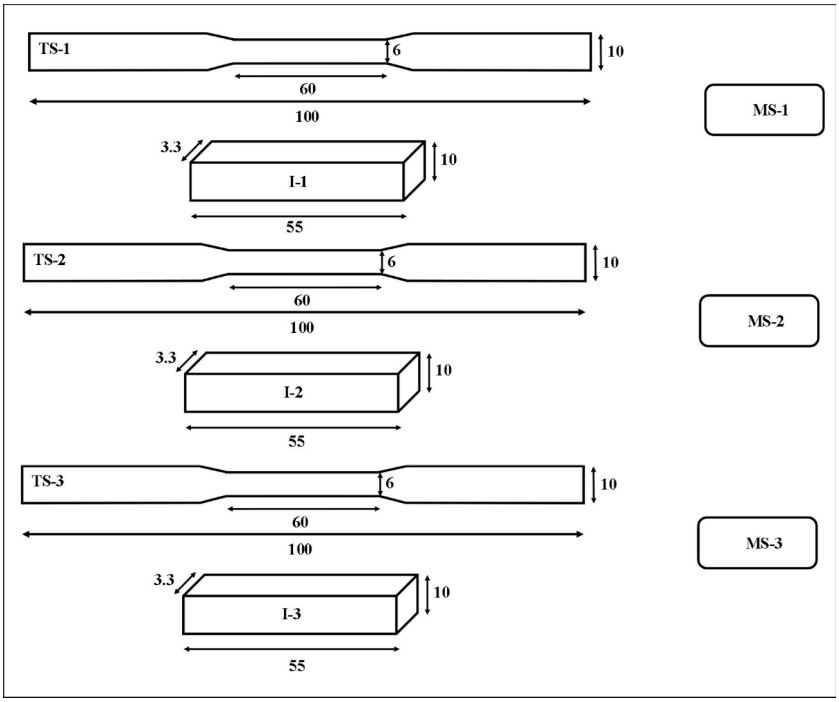

Fig. 2. Schematic of built structure representing the positions of testing specimens.

microstructure has been carried out by using an optical microscope (RADICAL instrument).

Mechanical investigations of tensile testing, microhardness, impact test, and fractography have been conducted at three positions along the horizontal depositing direction. WEDM was used to prepare the specimens for tensile test as per ASTM E8M standard, and impact test. M-100 universal tensile test instrument was employed to evaluate the tensile properties of specimens. For the Charpy impact test, AIT-300 Charpy impact was utilized to evaluate their properties. Locations of tensile and impact specimens are depicted in Fig. 2. All the dimensions shown in Fig. 2 are in mm.

A Vicker microhardness tester (ESEWAY EW-150) was employed to record the MH of the wall structure as per the ASTM E384 standard. A load of 150 gf with 10 s of dwell time was implemented during each MH measurement. MH readings were recorded at multiple positions. Three indentations at every location were applied and their mean value was taken for analysis. The fractography of the tensile and impact specimens was observed through Scanning electron microscopy (Zeiss Ultra 55).

Results and discussion

Fabrication of wall structure

The fabrication of wall structure along with their desired mechanical characteristics is considered to be essential which can be obtained at suitbale optimized set of WAAM variables. The wall structure of SS309L as shown in Fig. 3 has been successfully fabricated on the SS316L substrate plate at optimal parametric settings. The optimal process parameters include voltage at 22 V, gas mixture ratio of 3, travel speed of 20 mm/s, gas flow rate of 15 L/min, arc length of 3 mm, and deposition length of 150 mm. The layer-on-layer deposition of wall structure has been manufactured by using 180° turns of SS309L wire to obtain better precision. Identical layer-on-layer deposition can be seen for the wall structure. In between the bead-on-bead depositions, seamless fusion was observed. The built component was also found to be free from disbinding. A few lumps of metallic wire of SS309L can be seen on the sides of the built component. However, they have been successfully removed in post-processing. Thus, the optimal parametric setting was successful

Fig. 3. Wall structure of SS309L.

in manufacturing the wall structure of SS309L. The microstructure and mechanical characteristics of the wall structure have been investigated at three positions as shown in Fig. 2 along the depositing direction.

Microstructure

The microstructure of the wall structure is as shown in Fig. 4a–c. The most important factor in determining the microstructure of the steel is its cooling rates (Matlock et al., 2020). Here, all the layers of the built part experiences different heating and cooling rates. Hence the microstructure has been developed for three different zones namely (top layer, middle layer and bottommost layer). When the part is additively manufactured, the first layer (bottom most layer) deposited on the plate, experiences extreme cooling rates owing to cold surroundings and the

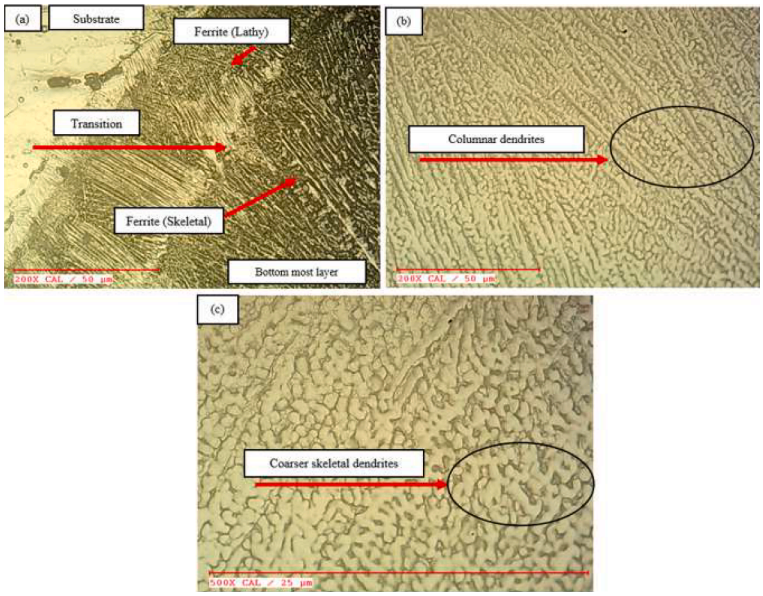

Fig. 4. Microstructure at (a) bottom, (b) middle, and (c) top section of built wall.

substrate plate (Li et al., 2015). The resultant microstructure as shown in Fig. 4a are skeletal ferrites. The atoms during cooling are given lesser time for rearrangement. Hence, a fine granular structure is seen in addition to colony of columnar dendrites. Similar results very observed by other researchers (Vora et al., 2022; Lee, 2020) wherein they also used GMAW to deposited SS. A planar microstructure is seen on one side which the substrate plate and a transition thereon. The microstructure image of Fig. 4c shows the features of topmost or the last layer of the additively manufactured component. A mix of dendritic structure with even coarser structures have been found. This is because of continuous heat built up and relatively slower cooling rates as compared to previous layers (Gao et al., 2019).

Mechanical properties

This section represents the obtained results and discussions of mechanical investigation. To obtain precise and reproducible results, three samples were tested, and average value has been considered during the analysis.

Microhardness tesing

A Vicker microhardness tester (ESEWAY EW-150) was employed to record the MH of the wall structure as per the ASTM E384 standard. MH readings were recorded at three locations and at every location, five indentations were applied and their mean value was taken for analysis. Fig. 5 depicts the MH measured at three locations. The mean value of MH was observed to be 159 ± 4.21 HV, 162 ± 3.89 HV 168 ± 5.34 HV for the top, middle, and bottom sections respectively. The top section had having marginally lower value of MH than the bottom, and middle sections. This was because the bottom zone has initial layers of wall structure and the heat-affected zone. The microstructure study has shown finer grain size for midde zone in comparison with top section, thus middle section is little harder than the top. Due to this reason, top section has resulted in least MH value. The obtained finding was in correlation with the results presented by Gao et al. (2019) and Wu et al. (2019). However, the values do not depict a significant variation (less than 5 %), so they were considered to be uniform. Therefore, the uniform MH also confirmed that the component will not have brittle failure.

Tensile strength

Tensile testing of the wall structure has been carried out in top (TS-1), middle (TS-2), and bottom sections (TS-3). Before the fracture, all the tested samples showed elastic and plastic deformation. Table 3 depicts the derived results from the test which has shown TS-1, TS-2, and TS-3 of 417 MPa, 409 MPa, and 402 MPa for yield strength (YS) respectively. Ultimate tensile strength (UTS) of 563 MPa, 556 MPa, 551 MPa, and percentage elongation for TS-1, TS-2, and TS-3 of 42 %, 38 %, 39 % were recorded for TS-1, TS-2, and TS-3 respectively. The tensile strength of all three positions has shown the least deviations across the built structure. The top section has experienced comparatively higher strength than the middle and bottom. This was due to the lower cooling rate of top section

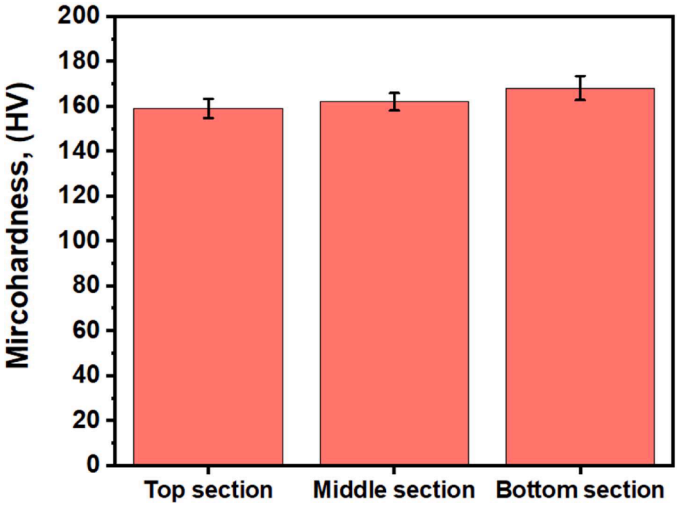

Fig. 5. Microhardness across the wall structure.

Table 3
Summary of tensile properties of wall structure of SS309L and wrought 309 L.

Specimen/Properties	YS, (MPa)	UTS, (MPa)	EL, (%)
hTS-1 (Top section)	417	563	42
hTS-2 (Middle section)	409	556	38
hTS-3 (Bottom section)	402	551	39
Average	409.33 ± 7.66	556.66 ± 6.33	39.66 ± 2.33
Wrought 309L	360–480	530–650	35–45

owing to the formation of succeeding layers of depositions. However, the values do not depict a significant variation, so they were considered to be uniform. It also confirms the identical deposition through the component. Thus, identical deposition with a favourable tensile strength of components suggested the suitability of the used process for the fabrication of the wall structure. The mean value of YS, UTS, and elongation for wall structure depicted the values of 409.33 ± 7.66 MPa, 556.66 ± 6.33 MPa, and 39.66 ± 2.33 %. Fig. 6 shows the graphical representation of these average values. The wrought 309 L steel has tensile strengths in the range of 360–480 MPa for YS, 530–650 MPa for UTS, and 35–45 % elongation. The obtained results of tensile strength of the wall structure fall in the range of tensile strength as that of wrought 309 L steel. This confirms the quality of the wall structure was found to be suitable for industrial applications of SS309L (Chen et al., 2018). Mai et al. (2021) have reported similar findings for WAMM of 308 L components.

The fracture surface morphology of the tensile test specimen depicted in Fig. 7 was analyzed through an SEM machine. Fig. 7 depictsed multiple dimples on the surface of fracture parts with homogenous distribution. This demonstrates the good toughness of the built component (Zhang et al., 2014). Additionally, the availability of extensive dimples demonstrated suitable ductility of the muti-walled component.

Impact testing

For the Charpy impact test, AIT-300 Charpy impact was utilized to evaluate their properties. For the top section, middle section, and bottom sections, the results depicted the values of 23.9 J, 24.6 J, and 25.7 J, respectively. Fig. 8 shows the graphical representation of these values. It has shown the mean impact test result of value 24.7 J. Thus, the obtained results have shown good strength in comparison with the strength of wrought SS309L. Impact test results have shown negligible deviation. The top section had having marginally lower value than the bottom section, and middle section. This was due to the higher cooling rate of the bottom section owing to the atmosphere and colder plate. However, the values don't depict a significant variation, so they were considered to be uniform. Thus, the outcome recommended the adequacy of the used method to manufacture wall structure along with the required properties.

SEM was employed to assess the fracture surface morphology of the impact test specimen as shown in Fig. 9. The occurrence of multiple dimples on the fracture surface has confirmed the ductile behaviour, and their homogenous distribution revealed the superior ductility of the built wall structure (Kumar et al., 2021).

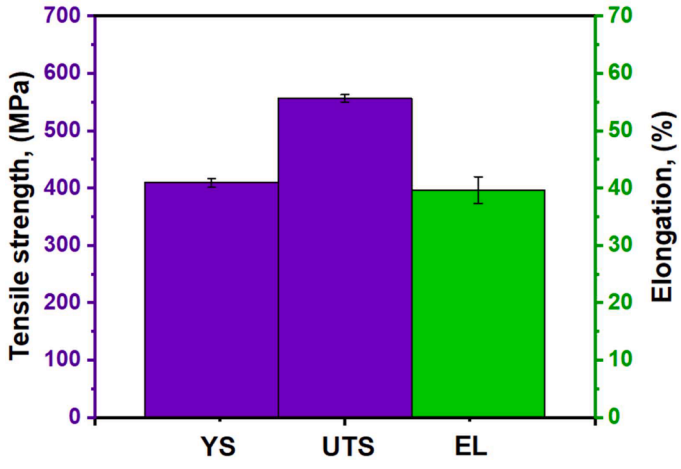

Fig. 6. Tensile strength of the wall structure at different locations.

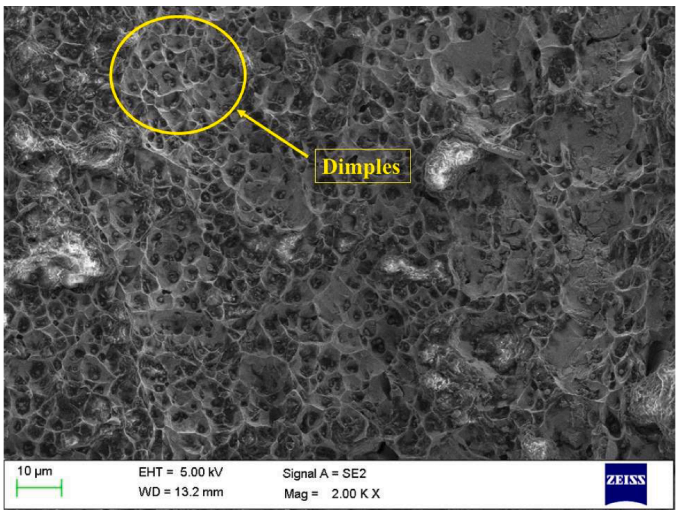

Fig. 7. Fracture surface morphology of tensile test specimen.

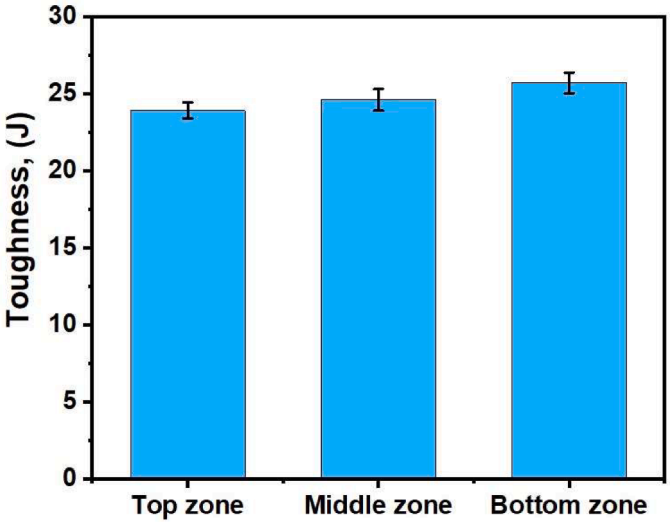

Fig. 8. Results of impact test of the wall structure at different locations.

Conclusion

In the present study optimized parametric settings obtained through the PVS algorithm were employed to fabricate a defect-free structure. A wall structure of SS309L was built on the SS316L substrate plate by employing the GMAW based WAAM process. Based on the obtained results, the following conclusions were drawn:

- The wall structure of SS309L was effectively manufactured by using optimized set of variables. The optimal parametric settings for fabrication of wall structure was effective as it wall structure was observed without any disbonding along with seamless fusion among the bead-on-bead depositions.
- Microstructure study has shown a fine granular structure in addition to colony of columnar dendrites in bottom section, a columnar dendrites in middle section, and a mix of dendritic structure with even coarser structures in top section.
- Mechanical investigations of tensile testing, microhardness, impact test, and fractography have been conducted at three positions (top, middle and bottom). The average value of microhardness was recorded as 159 ± 4.21 HV, 162 ± 3.89 HV 168 ± 5.34 HV for the top, middle, and bottom sections respectively. The uniform MH

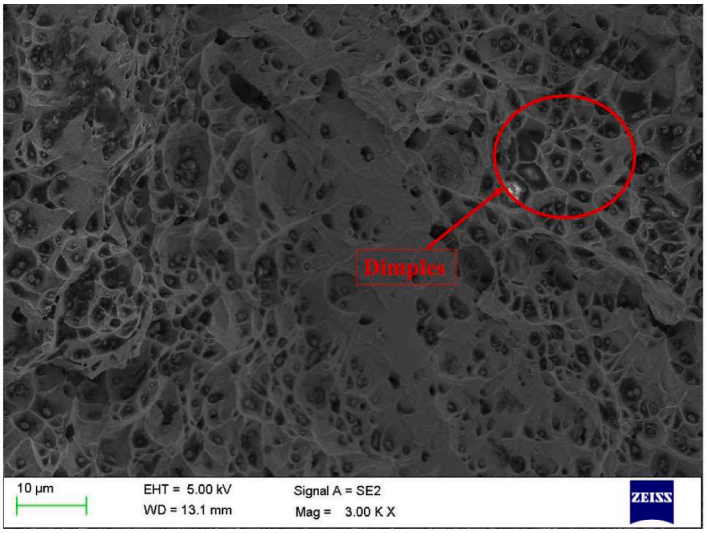

Fig. 9. Fracture surface morphology of impact test specimen.

values also confirmed that the component will not have brittle failure.

- For the top section, middle section, and bottom sections, the results depicted the values of 23.9 J, 24.6 J, and 25.7 J, respectively. It has shown the mean impact test result of value 24.7 J. Therefore, the obtained result of the impact test for wall structure has shown good strength in comparison with the strength of wrought SS309L.
- The tensile strength for the wall structure has shown mean values of YS, UTS, and elongation to be 409.33 ± 7.66 MPa, 556.66 ± 6.33 MPa, and 39.66 ± 2.33 % respectively. The wrought 309 L steel has tensile strengths in the range of 360–480 MPa for YS, 530–650 MPa for UTS, and 35–45 % elongation. Thus, the obtained results of the tensile strength of the wall structure fall in the range of tensile strength as that of wrought 309 L steel.
- Fractography of the tensile and impact specimens obtained through SEM has revealed the superior ductility for the built structure as fractured surface was observed to have multiple dimples. Thus, the outcome recommended the adequacy of GMAW based WAAM method to manufacture multi-layered specimens along with the required properties.
- The obtained results were found to be vital for various industrial applications and also useful in case of conducting further research in the domain. The current study paves way for the successful implementation of WAAM technique for manufacturing of SS309L components particularly for critical applications such as nuclear reactors, powerplant valves/flanges etc. One of the key application of the study is also repair of existing broken or damaged parts rather than replacing them entirely.

CRediT authorship contribution statement

Rakesh Chaudhari: Conceptualization, Data curation, Investigation, Methodology, Writing – original draft. **Sakshum Khanna:** Formal analysis, Investigation, Methodology. **Jay Vora:** Resources, Supervision. **Vivek Patel:** Supervision, Writing – review & editing.

Declaration of Competing Interest

The authors declare that they have no known competing financial interests or personal relationships that could have appeared to influence the work reported in this paper.

Data availability

No data was used for the research described in the article.

References

Babu, A., et al., 2023. Local control of microstructure and mechanical properties of high-strength steel in electric arc-based additive manufacturing. J. Mater. Res. Technol. 26, 1508–1526.
Bajaj, P., et al., 2020. Steels in additive manufacturing: a review of their microstructure and properties. Mater. Sci. Eng. A 772, 138633.
Chaudhari, R., et al., 2022b. Parametric study and investigations of bead geometries of GMAW-based Wire–Arc Additive Manufacturing of 316L stainless steels. Metals (Basel) 12 (7), 1232.
Chaudhari, R., et al., 2022a. Effect of multi-walled structure on microstructure and mechanical properties of 1.25 Cr-1.0 Mo steel fabricated by GMAW-based WAAM using metal-cored wire. J. Mater. Res. Technol. 21, 3386–3396.
Chaudhari, R., et al., 2023. A parametric study and experimental investigations of microstructure and mechanical properties of multi-layered structure of metal core wire using wire arc additive manufacturing. J. Adv. Join. Process. 8, 100160.
Chen, X., et al., 2018. Effect of heat treatment on microstructure, mechanical and corrosion properties of austenitic stainless steel 316L using arc additive manufacturing. Mater. Sci. Eng. A 715, 307–314.
Derekar, K., 2018. A review of wire arc additive manufacturing and advances in wire arc additive manufacturing of aluminium. Mater. Sci. Technol. 34 (8), 895–916.
Dinovitzer, M., et al., 2019. Effect of Wire And Arc Additive Manufacturing (WAAM) process parameters on bead geometry and microstructure. Addit. Manuf. 26, 138–146.
Duarte, V.R., et al., 2021. Wire and arc additive manufacturing of high-strength low-alloy steel: microstructure and mechanical properties. Adv. Eng. Mater. 23 (11), 2001036.
Gao, C., et al., 2019. Location dependence of microstructure and mechanical properties on wire arc additively manufactured nuclear grade steel. Vacuum 168, 108818.
Hu, Z., et al., 2020. Multi-bead overlapping model with varying cross-section profile for robotic GMAW-based additive manufacturing. J. Intell. Manuf. 31 (5), 1133–1147.
Ilman, M.N., Widodo, A., Triwibowo, N., 2022. Metallurgical, mechanical and corrosion characteristics of vibration assisted gas metal arc aa6061-T6 welded joints. J. Adv. Join. Process. (6), 100129
Isquierdo, D., et al., 2022. Effect of the initial substrate temperature on heat transfer and related phenomena in austenitic stainless steel parts fabricated by additive manufacturing using direct energy deposition. J. Mater. Res. Technol. 18, 5267–5279.
Israr, R., Buhl, J., 2023. An Additive Introduction Manufacturing to (AM) of metals and its trends in Wire-Arc Additive Manufacturing (WAAM) simulations. Machine Tools: An Industry 4.0 Perspective, p. 103.
Ji, L., et al., 2017. Microstructure and mechanical properties of 304L steel fabricated by arc additive manufacturing. In: MATEC Web of Conferences. EDP Sciences.
Jin, W., et al., 2020. Wire arc additive manufacturing of stainless steels: a review. Appl. Sci. 10 (5), 1563.
Kimura, M., et al., 2020. Effects of tensile strength on friction welding condition and weld faying surface properties of friction welded joints between pure copper and austenitic stainless steel. J. Adv. Join. Process. (2), 100028
Kokare, S., et al., 2023. Environmental and economic assessment of a steel wall fabricated by wire-based directed energy deposition. Addit. Manuf. 61, 103316.

Korkmaz, M.E., et al., 2022. A technical overview of metallic parts in hybrid additive manufacturing industry. J. Mater. Res. Technol.
Kumar, D., et al., 2021b. Mechanisms controlling fracture toughness of additively manufactured stainless steel 316L. Int. J. Fract. 1–18.
Kumar, V., et al., 2021a. Parametric study and characterization of wire arc additive manufactured steel structures. Int. J. Adv. Manuf. Technol. 115 (5–6), 1723–1733.
Lee, S.H., 2020. CMT-based wire arc additive manufacturing using 316L stainless steel: effect of heat accumulation on the multi-layer deposits. Metals 10 (2), 278.
Li, K., et al., 2015. Microstructure evolution and mechanical properties of multiple-layer laser cladding coating of 308L stainless steel. Appl. Surf. Sci. 340, 143–150.
Li, S.-H., et al., 2023. Directed energy deposition of metals: processing, microstructures, and mechanical properties. Int. Mater. Rev. 68 (6), 605–647.
Mai, D.S., 2020. Microstructural and mechanical characteristics of 308L stainless steel manufactured by gas metal arc welding-based additive manufacturing. Mater. Lett. 271, 127791.
Mai, D.S., Doan, T.K., Paris, H., 2021. Wire and arc additive manufacturing of 308L stainless steel components: optimization of processing parameters and material properties. Eng. Sci. Technol. Int. J. 24 (4), 1015–1026.
Matlock, D.K., et al., 2020. Applications of rapid thermal processing to advanced high strength sheet steel developments. Mater. Charact. 166, 110397.
Müller, J., Hensel, J., Dilger, K., 2022. Mechanical properties of wire and arc additively manufactured high-strength steel structures. Weld. World 1–13.
Nguyen, H.D., et al., 2022. A critical review on additive manufacturing of Ti-6Al-4V alloy: microstructure and mechanical properties. J. Mater. Res. Technol. 18 (4641), e4661.
Piscopo, G., Iuliano, L., 2022. Current research and industrial application of laser powder directed energy deposition. Int. J. Adv. Manuf. Technol. 119 (11–12), 6893–6917.
Rauch, M., Nwankpa, U.V., Hascoet, J.-Y., 2021. Investigation of deposition strategy on wire and arc additive manufacturing of aluminium components. J. Adv. Join. Process. 4, 100074.
Shen, B., et al., 2022. Multimodal-based weld reinforcement monitoring system for wire arc additive manufacturing. J. Mater. Res. Technol.
Sinha, A.K., Pramanik, S., Yagati, K.P., 2022. Research progress in arc based additive manufacturing of aluminium alloys-a review. Measurement, 111672.
Sohrabi, M.J., Naghizadeh, M., Mirzadeh, H., 2020. Deformation-induced martensite in austenitic stainless steels: a review. Arch. Civil Mech. Eng. 20, 1–24.
Taheri, H., et al., 2022. Assessment of material property variations with resonant ultrasound spectroscopy (RUS) when using additive manufacturing to print over existing parts. J. Adv. Join. Process. 5, 100117.
Van, T.L., et al., 2021. Wire and arc additive manufacturing of 308L stainless steel components: optimization of processing parameters and material properties. Eng. Sci. Technol. Int. J. 24 (4), 1015–1026.
Van Thao, L., 2020. A preliminary study on gas metal arc welding-based additive manufacturing of metal parts. VNUHCM J. Sci. Technol. Dev. 23 (1), 422–429.
Vora, J., et al., 2022b. Experimental investigations on mechanical properties of multi-layered structure fabricated by GMAW-based WAAM of SS316L. J. Mater. Res. Technol. 20, 2748–2757.
Vora, J., et al., 2022a. Optimization of bead morphology for GMAW-based Wire-Arc Additive Manufacturing of 2.25 Cr-1.0 Mo steel using metal-cored wires. Appl. Sci. 12 (10), 5060.
Vora, J., et al., 2023. Fabrication of multi-walled structure through parametric study of bead geometries of GMAW-based WAAM process of SS309L. In: Materials, 16, p. 5147.
Wang, D., et al., 2019. The effects of fabrication atmosphere condition on the microstructural and mechanical properties of laser direct manufactured stainless steel 17-4 PH. J. Mater. Sci. Technol. 35 (7), 1315–1322.
Williams, S.W., et al., 2016. Wire+ arc additive manufacturing. Mater. Sci. Technol. 32 (7), 641–647.
Wu, B., et al., 2018. A review of the wire arc additive manufacturing of metals: properties, defects and quality improvement. J. Manuf. Process. 35, 127–139.
Wu, W., et al., 2019. Forming process, microstructure, and mechanical properties of thin-walled 316L stainless steel using speed-cold-welding additive manufacturing. Metals 9 (1), 109.
Zahidin, M.R., et al., 2023. Research challenges, quality control and monitoring strategy for Wire Arc Additive Manufacturing. J. Mater. Res. Technol.
Zhang, D., et al., 2022. Additive manufacturing of duplex stainless steels-a critical review. J. Manuf. Process. 73, 496–517.
Zhang, K., et al., 2014. Characterization of stainless steel parts by laser metal deposition shaping. Mater. Des. 55, 104–119.
Zhou, J., Barrett, R.A., Leen, S.B., 2022. Three-dimensional finite element modelling for additive manufacturing of Ti-6Al-4V components: effect of scanning strategies on temperature history and residual stress. J. Adv. Join. Process. 5, 100106.